



**HAL**  
open science

## Meso/macro scale response of the comingled glass polypropylene 2-2 twill woven fabric under shear pre-tension coupling

Ming Mei, Yujia He, Xujing Yang, Kai Wei, Fuhao Mo

► **To cite this version:**

Ming Mei, Yujia He, Xujing Yang, Kai Wei, Fuhao Mo. Meso/macro scale response of the comingled glass polypropylene 2-2 twill woven fabric under shear pre-tension coupling. *Composite Structures*, 2020, 236, pp.111854. 10.1016/j.compstruct.2020.111854 . hal-03240320

**HAL Id: hal-03240320**

**<https://amu.hal.science/hal-03240320>**

Submitted on 28 May 2021

**HAL** is a multi-disciplinary open access archive for the deposit and dissemination of scientific research documents, whether they are published or not. The documents may come from teaching and research institutions in France or abroad, or from public or private research centers.

L'archive ouverte pluridisciplinaire **HAL**, est destinée au dépôt et à la diffusion de documents scientifiques de niveau recherche, publiés ou non, émanant des établissements d'enseignement et de recherche français ou étrangers, des laboratoires publics ou privés.



Distributed under a Creative Commons Attribution - NonCommercial - NoDerivatives 4.0 International License

**Meso/macro scale response of the comingled glass polypropylene 2-2  
twill woven fabric under shear pre-tension coupling**

Ming Mei<sup>1</sup>, Yujia He<sup>1</sup>, Xujing Yang<sup>1</sup>, Kai Wei<sup>1, 2, \*</sup>, Fuhao Mo<sup>1, 3, \*\*</sup>

<sup>1</sup> State Key Laboratory of Advanced Design and Manufacture for Vehicle Body,  
Hunan University, Changsha, Hunan 410082, China

<sup>2</sup> State Key Laboratory of Structural Analysis for Industrial Equipment, Dalian  
University of Technology, Dalian, 116024, PR China

<sup>3</sup>Aix-Marseille University, IFSTTAR, LBA UMRT24, Marseille, France

\*Corresponding author E-mail: [weikai@hnu.edu.cn](mailto:weikai@hnu.edu.cn) (Kai Wei)

\*\*Corresponding author E-mail: [fuhaomo@hnu.edu.cn](mailto:fuhaomo@hnu.edu.cn) (Fuhao Mo)

**Abstract:** Pre-tension is well known as an effective approach to suppress forming defects caused by excessive shearing in manufacture process of the fabric reinforced composites. While, the coupling between shear and pre-tension of the fabrics is not thoroughly understood. Here, this work aims to explore and understand the meso/macro scale response of the comingled glass-polypropylene 2-2 twill woven fabric under shear pre-tension coupling. A self-developed picture frame fixture including a concise approach to apply pre-tension in shear experiments of the fabric was originally developed. Then, systematical shear experiments confirm that the critical shear angle of the fabric is  $40^\circ$ , as the fabric suffers in-plane complex deformations when the shear angle is above  $40^\circ$ . Additionally, the pre-tension significantly enlarges the shear force when the shear angle is lower than critical value of  $40^\circ$ . In view of mesoscopic scale, the pre-tension suppresses the undulation of the un-sheared fabric surface, revealing an enhancement of the coupling effect at the initiation of the shear deformation. Besides, the pre-tension also reduces the variation of yarn width. While, these mesoscopic effects caused by pre-tension are not pronounced when it is higher than 1.2N/mm. The devised picture frame fixture and the exploration of the shear pre-tension coupling behavior provide an important experimental basis to the purpose of suppressing forming defect and to raise the manufacture efficiency of the fabric reinforced composites.

**Keywords:** Fabrics; Composite; Picture frame; Shear-tension coupling; Forming defect

## 1 Introduction

Due to the high strength/stiffness, low density and high manufacture flexibility, continuous fiber fabric reinforced resin matrix composites are widely used in vehicle engineering, especially in new energy vehicles for weight saving consideration [1-4]. It is well known that the preforming of the continuous fiber fabric is an important step in manufacture process of the composites, and the defects such as wrinkle in fabrics generated in the manufacture process have significant negative influence on the overall mechanical properties [5, 6].

As indicated in reported literature, tensile, in-plane shear and bending are the primary deformation modes of the continuous fiber fabric in the forming process. Specially, in-plane excessive shearing, which is mainly related to the initiation of wrinkles defect [7-13], and significantly affects the fabric permeability [14, 15] in liquid composite molding (LCM) process, is considered as the most dominant deformation mode [16-19]. Thus, in order to explore the shear behavior of the fabrics, the picture frame and the bias extension tests are widely reported in literature [10-12]. Fig. 1 illustrates the basic principles of these two testing protocols. Compared with the bias extension test, the superiority of the picture frame test is that it can provide relative more uniform shear deformation field without slippage of the yarns [20, 21].

Besides the exploration of the shear experiments, actually, a number of works reported that applying pre-tension to fabrics through such as blank holder [22-25] and spring-load clamps [26, 27] was an effective way to suppress wrinkles caused by excessive shearing. Thus, recently, several studies discussed the shear pre-tension

coupling properties of the fabrics through the picture frame testing devices [28-31]. For instance, Willems et al. [28] revealed that the shear resistance increased with the enlarged pre-tension. Launay et al. [29] confirmed that the shear force was affected by the membrane pre-tension induced by the different clamping of fabric on the picture frame devices. Nosrat-Nezami et al. [30] utilized air cylinders to apply constant pre-tension force, and indicated that the shear force was affected by the membrane pre-tension in the whole shearing process. Haghi Kashani et al. [31] reported that the shear force of the fabric inclined with the increasing pre-tension provided by the displacement control at the initial shear angle. While, the distinctions of the shear force under different pre-tensions were not obvious at high shear angle due to the relaxation of the pre-tension on the fabric.

It should be well noted that the above studies on shear pre-tension coupling behavior of the fabric mainly focus on the characterization of macro performance including such as shear force versus angle curves and shear deformations. Actually, the evolution of mesoscopic feature of fabric such as yarn width is a key factor in the formation of wrinkle defects in the shear deformation. While, up to now, the studies on the yarn width evolution are carried out in the shear test without applying pre-tension [11, 12]. That is the effects of applying pre-tension on the yarn width evolution in the shear deformation have not been revealed yet.

Thus, the objective of this paper is to explore the effects of the pre-tension on the shear behavior of a typical kind of fabric, namely, the comingled glass-polypropylene 2-2 twill woven fabric in view of both macro and mesoscopic scales. As the necessary

experimental basis, a self-developed picture frame fixture, which included a relatively concise approach to apply pre-tension loading, was originally designed. Then, the shear experiments under different levels of pre-tension were conducted, and the macroscopic shear force and shear deformation of the fabric were discussed. Finally, the mesoscopic features in shear pre-tension coupling deformation, including undulation of fabric surface and variation of yarn width, were analyzed and discussed. Then, the devised picture frame fixture and the exploration of the shear pre-tension coupling behavior provide an important experimental basis to the purpose of suppressing forming defect.

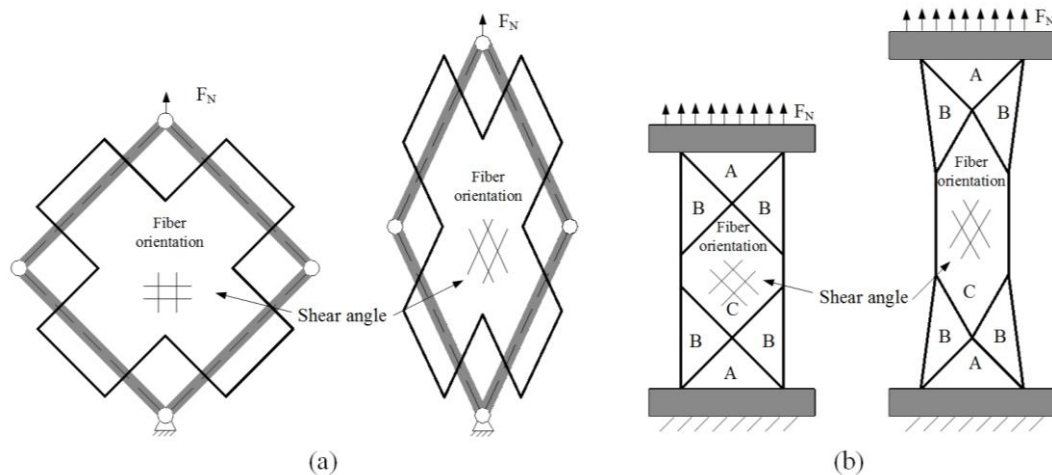


**Fig. 1** Two protocols commonly used to characterize shear behavior of the fabrics: (a) picture frame and (b) bias extension tests.

## 2 Experiments

### 2.1 Fabric and sample preparation

As shown in Fig. 2a, the comingled glass-polypropylene 2-2 twill woven fabric, which is widely used in vehicle engineering, is selected as a representative for shear pre-tension coupling tests in this work. The fabric is composed of 60% E-glass fiber

and 40% polypropylene fiber. It can be seen that the woven tightness of the selected fabric is large, and the basic specification and geometrical properties are listed in Table 1. As illustrated in Fig. 2b, the cross shape sample was designed and prepared before tests. The shear region in the middle of the sample was 100 mm × 100 mm. Considering the effects of the local bending of yarns closed to the clamp induced by the clamp design on the pure shear deformation of the shear region, the rovings, which were adjacent to the shear region, were removed to reduce boundary effect according to the reported literature [11]. Additionally, the distance between the shear region and the clamp was enhanced to be 55mm to reduce the boundary effect on the center shear region. In order to measure the full-field deformation by the digital image correlation (DIC) method, in the pre-treatment, black dots were uniformly marked on the surface of shear region.

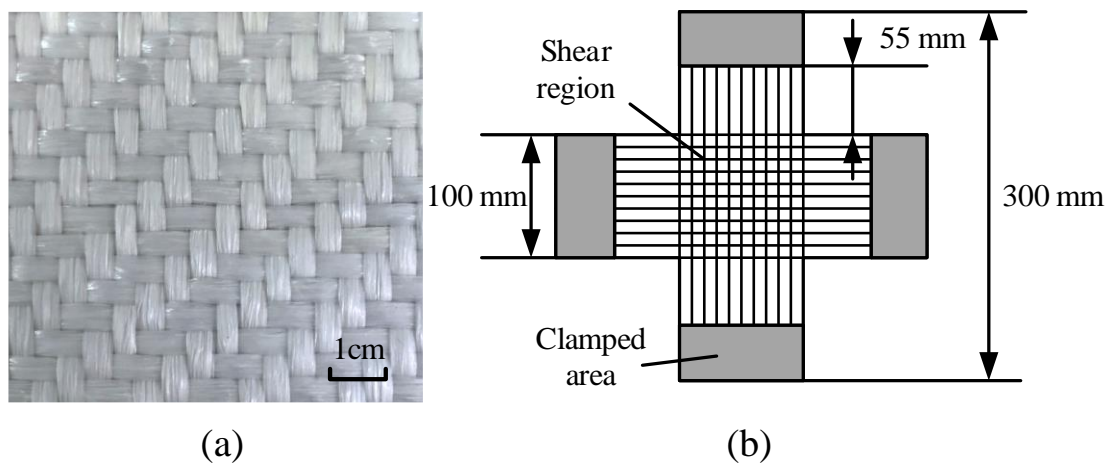


**Fig. 2** (a): the comingled glass-polypropylene fabrics and (b): schematic diagram of the sample.

**Table 1** Specification and geometrical properties of the comingled glass-polypropylene fabrics.

Weight fraction (glass)	Area density (g/m <sup>2</sup> )	Yarn linear density (tex)	Thickness (mm)	Yarn spacing (mm)	Yarn width (mm)
60%	950	1870	1.4	4.9	4.17

## 2.2 Picture frame fixture

Currently, the shear pre-tension coupling behavior was investigated by the developed picture frame fixture, which is composed of the traditional picture frame fixture and the applying pre-tension device [29-31]. The current applying pre-tension devices mainly utilized the cylinder or motor to provide pre-tension, and measured the pre-tension value by the sensor, which usually require various equipments, and are costly. Thus, in this work, similarly, a picture frame fixture was originally developed by mechanical structural design to test the shear pre-tension coupling behavior of the fabrics. Especially, different from the reported picture frame fixtures [29-31], here, the designed picture frame fixture with the springs is relatively concise and convenient to apply pre-tension. As shown in Fig. 3, the fixture includes two parts: a tension exerting and a picture frame for shear exertion. The picture frame part consists of four high strength aluminum (A7075) bars, which were connected via four hinge joints. The hinge joints were machined with high precision to reduce friction. The high strength aluminum was used to avoid the intrinsic deformation of the fixture and to minimize the weight for convenient operation.

The tension exerting part contains adjusting bolts, clamp plates, springs for exerting force, guide pillars and traction bars. The clamp plates and the traction bars were connected via four springs with a spring coefficient of 3.3 N/mm. The spring tension can be adjusted through the regulation bolt. A measure ruler is engraved on the side of tensioning bar to conveniently obtain a specific elongation of the springs (see Fig. 3). Two guide pillars were set to ensure smooth movement of the traction bars and clamp plates, in order to ensure uniform and parallel force. Fabric slip in test should be definitely avoided, thus, a rubber blanket was attached inside the clamp plates, and a small circular groove was machined on the inside surface of the top clamp plate. An alternative connector manufactured by monomer casting nylon was designed to fit the adapters of different testing machines. According to above design, this picture frame fixture can be used to explore the effects of different pre-tension on the shear behavior of the fabric under a large range of testing shear angles.

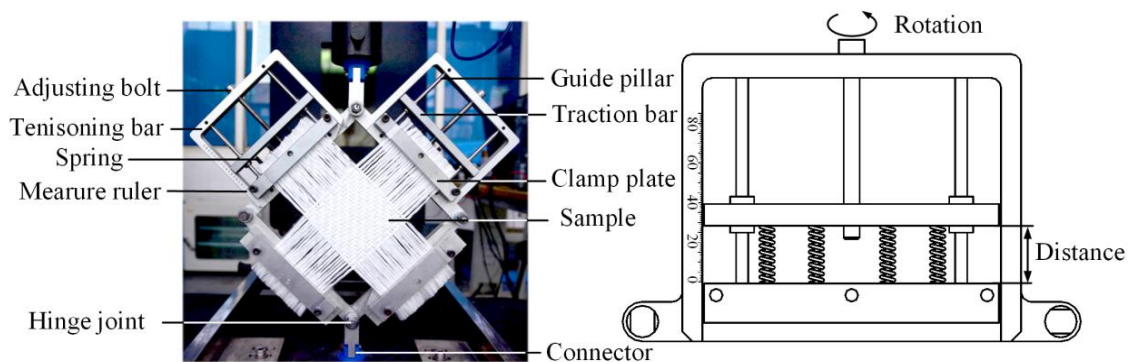


**Fig. 3** The self-developed picture frame fixture to test the shear pre-tension coupling behavior of the fabric.

### 2.3 Experimental procedure

In shear pre-tension coupling tests, this devised picture frame fixture was

installed in a universal testing machine (MTS E45.105). Shear tests were conducted on five levels of pre-tension including 0 N/mm, 0.6 N/mm, 1.2 N/mm, 1.8 N/mm and 2.4 N/mm. The loading speed is kept constant of 20 mm/min. For every pre-tension level, at least three repetitions were tested, and the averaged value was obtained for subsequent analysis.

The scheme of shear deformation mechanism in the fabric subjected to pre-tension is illustrated in Fig. 4. The parameters to characterize shear behavior under pre-tension is introduced as follow:  $F_N$  is the tensile force measured by the testing machine.  $F_{NS}$  is the normalized shear force in the fabric.  $F_T$  indicates the pre-tension force applied to fabric.  $L_{frame}$  is the distance between the adjacent rotatory joints.  $L_{fabric}$  is the sample's clamping length.  $d$  represents movement distance of the picture frame device along  $F_N$ .  $\theta$  is the angle between two bars.  $\lambda$  is the theoretical shear angle, and can be calculated by the geometric relationship:

$$\lambda = \frac{\pi}{2} - \theta = \frac{\pi}{2} - 2 \arccos\left(\frac{1}{\sqrt{2}} + \frac{d}{2L_{frame}}\right). \quad (1)$$

Generally, the normalized  $F_{NS}$  is calculated by [19]:

$$F_{NS} = \frac{F_N \cdot L_{frame}}{2 \cos\left(\frac{\theta}{2}\right) \cdot L_{fabric}^2}. \quad (2)$$

Similar to the reported literature [29, 31], due to the inherent characteristics of the devised picture frame fixture, it can be seen that the pre-tension  $F_T$  is applied by the springs, and the amplitude of the pre-tension remains constant since the variation of the springs' length is kept to be constant in tests. The direction of the pre-tension is also constantly along the spring direction, and is not along the yarn direction in tests.

Thus, this work investigates the effect of different levels of pre-tension on the shear behavior of the fabric.

The shear deformation process of the fabric was captured by a CCD and a camera(Point Grey GS3-PGE-91S6M; 9 million pixels; Resolution: 3376 x 2704) with a frequency of 1 frame/s. Then, the full-field displacement in shear process and the variation of fabric surface under different pre-tensions were calculated by digital image correlation software Vic 2D and Vic 3D, respectively. In order to obtain the yarn width at different shear angle, the corresponding pictures of shear deformation under specify shear angle captured by CCD were extracted and imported into ImageJ software. Then, the yarn width can be measured by the pixels, and the pixel value is converted to actual length using the scale bar. Finally, the yarn width was calculated by averaged value of 9 points randomly selected on three yarns to avoid the measurement error. Then, the variation of yarn width in shear process was also obtained.

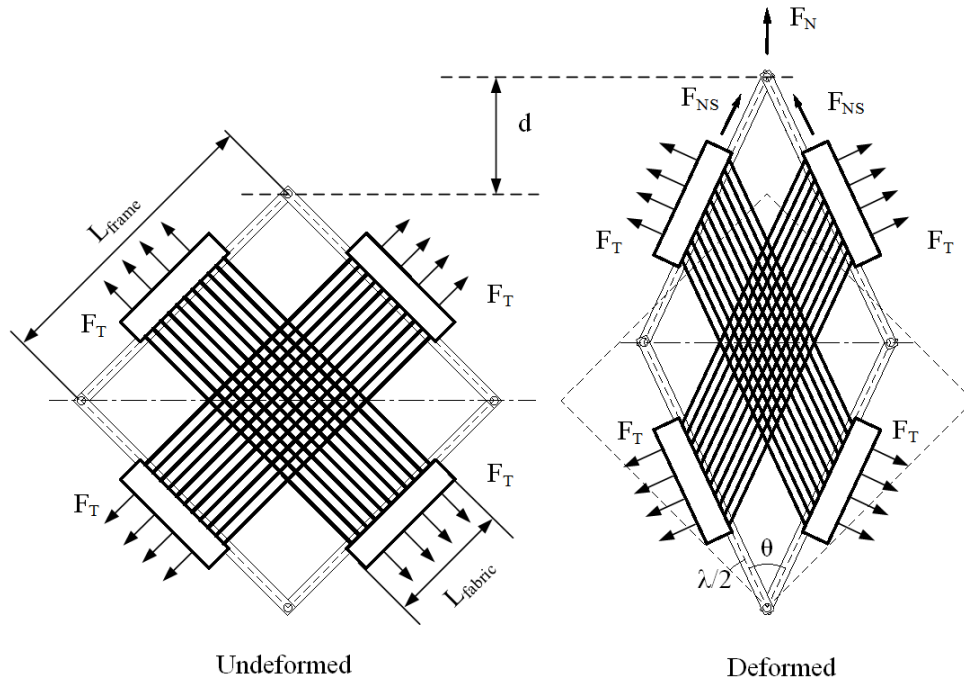


**Fig. 4** Schematic diagram of the coupling between the shear and pre-tension deformation in the picture frame fixture test.

### 3 Results

#### 3.1 Shear deformation

[Fig. 5](#) shows a typical full-field displacement contours at three shear angles ( $15^\circ$ ,  $30^\circ$  and  $45^\circ$ ) for a representative pre-tension of 2.4 N/mm. It is noted that the X displacements (absolute value) is symmetric with respect to the vertical diagonal line of the fabrics. Similarly, the Y displacement increases linearly from the bottom to top, and is also symmetric with respect to the vertical diagonal line. For instance, when the shear angle is  $45^\circ$ , the X placements of left and right symmetrical corner are of 199.4 and -199.225 pixels, respectively. The Y displacements of left and right symmetrical corner are of 445.105 and 445.602 pixels, respectively. These results indicate that a uniform shear deformation in the middle area of the sample is obtained, firmly demonstrating that the self-developed picture frame device can implement uniform

shear deformation under the applying pre-tension.

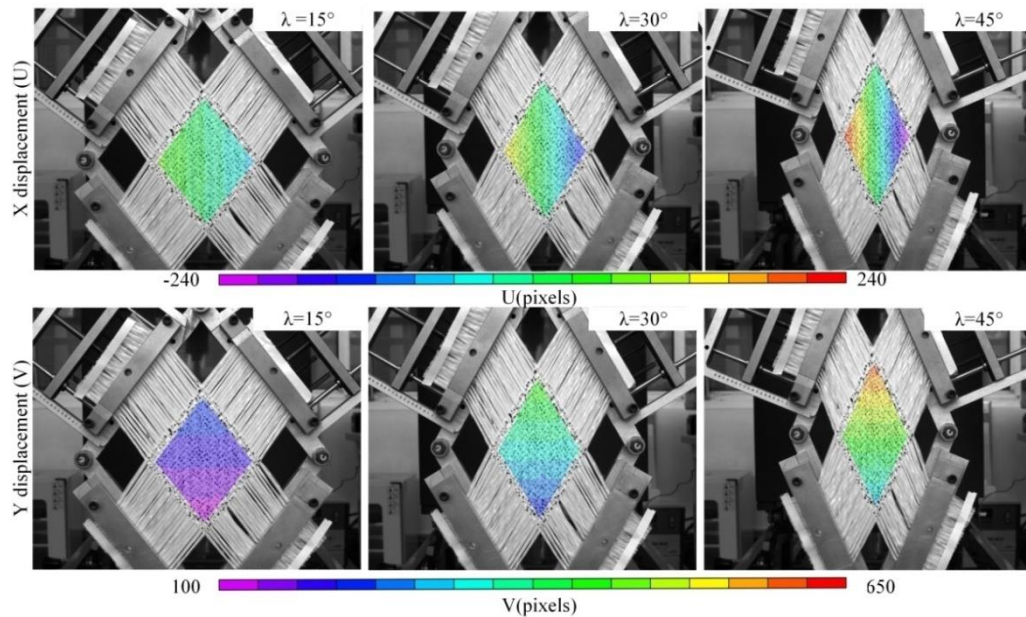


**Fig. 5** X and Y displacement in shear deformation under a typical pre-tension of 2.4 N/mm at three shear angles ( $15^\circ$ ,  $30^\circ$  and  $45^\circ$ ) obtained by DIC.

The comparison of practical shear angles measured by DIC results with the theoretical prediction by Eq. (1) is given in Fig. 6. It is noted that, generally, the measured shear angle is in agreement with theoretically calculated values under different pre-tensions in the considered range. While, when the theoretical shear angle is larger than  $40^\circ$ , the measured shear angle gradually becomes remarkably lower than theoretical ones, indicating that the shear deformation reaches a limit above this shear angle, and the deformation becomes non-pure in-plane shear behavior. This phenomenon can be also confirmed in Fig. 7.

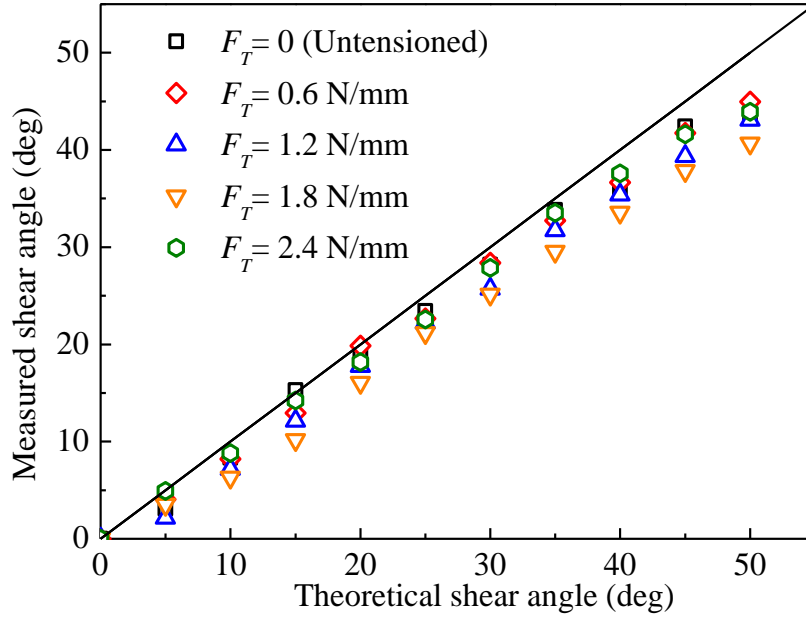


**Fig. 6** Comparison of the theoretically calculated shear angle with the measured shear angle under different pre-tensions.

As shown in Fig. 7, in order to compare the shear behavior before and after the shear limit, the local mesoscopic structure features before shear limit are extracted at shear angle of  $30^\circ$  and  $40^\circ$ , and the corresponding features after shear limit are extracted at shear angle of  $50^\circ$  to clearly reflect the variations. The points a, o, b are the intersections of weft yarn edge line and warp yarn edge line. The line oa and ob coincides with the edge of yarn at shear angle of  $30^\circ$  and  $40^\circ$  for all pre-tension levels, which means the fabric presents pure in-plane shear deformation, and demonstrates the sample design effectively limits the boundary effects. While, the line oa or ob is misaligned with the edges of yarn when the shear angle reaches large value of  $50^\circ$ , indicating that the in-plane shear deformation is not pure. Actually, the non-pure in-plane shear deformation at high shear angle of fabric is originated from the lateral

compression limitation of the yarn. Besides, the excessive lateral compression of the yarn induces the out of plane deformation, which can easily cause wrinkle defects in the forming process. Therefore, the non-pure in-plane shear deformation of fabric should be avoided in fabric forming process.

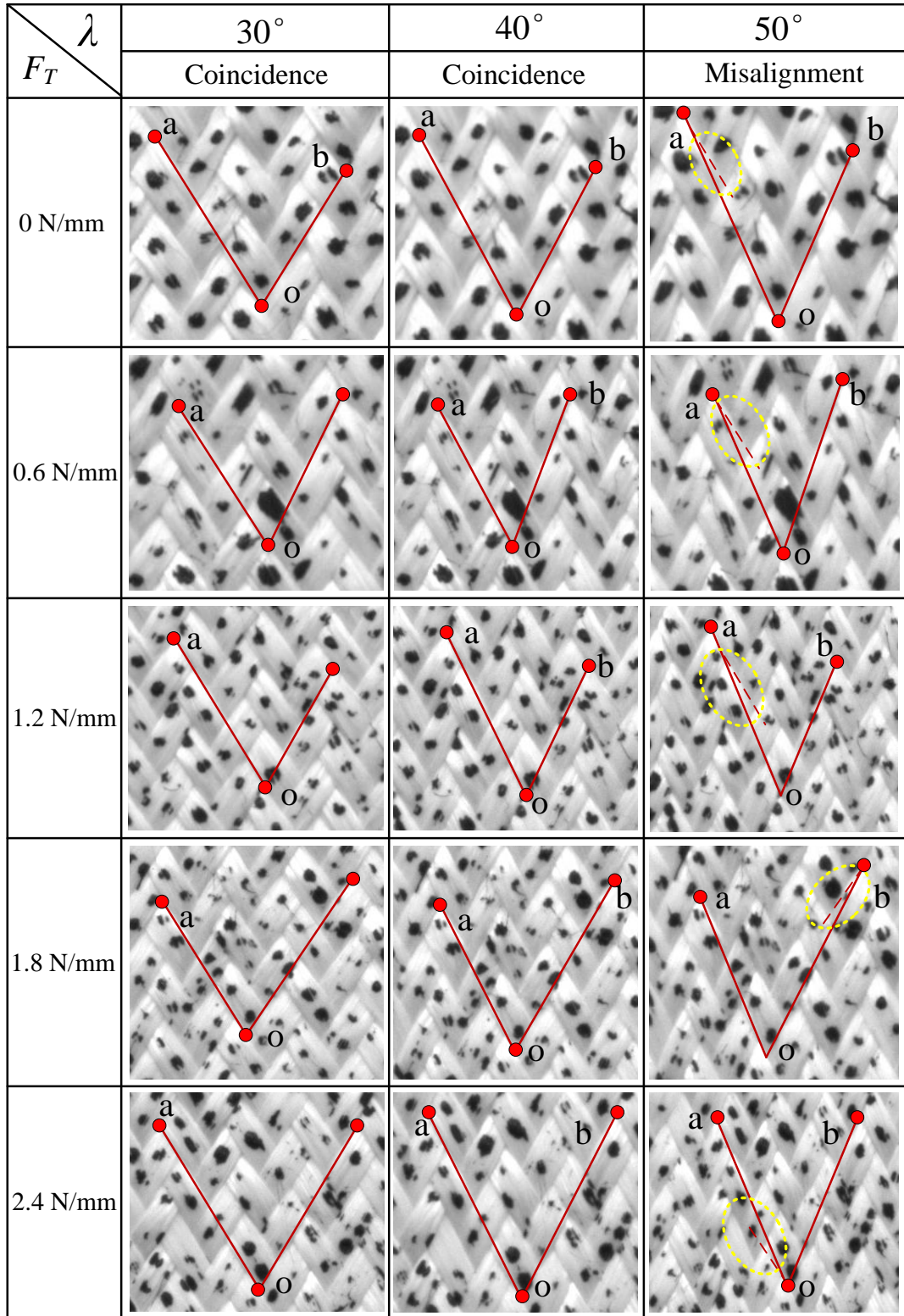


**Fig. 7** Mesoscopic structures of the fabric under shear deformation with different pre-tension at three shear angles (30°, 40° and 50°).

### 3.2 Effects of pre-tension on shear responses

According to Eq. (2), the normalized shear forces versus shear angles are shown in Fig. 8. It can be seen that the normalized shear forces rapidly rise when shear angle is higher than  $40^\circ$ , suggesting that this angle is a critical angle to determine the pure shear deformation limitation of this woven fabric, and wrinkle will be developed due to the densification (yarn locking) of woven fabric beyond this angle. When the shear angles lower than  $40^\circ$ . The normalized shear forces under pre-tension condition show evident enlargement compared with that without pre-tension. Typically, the values of normalized shear force at the shear angle of  $20^\circ$  are respectively 0.06 N/mm, 0.14 N/mm, 0.15 N/mm, 0.23 N/mm and 0.29 N/mm for the pre-tension levels of 0.0 N/mm, 0.6 N/mm, 1.2 N/mm, 1.8 N/mm and 2.4 N/mm. This result indicates that pre-tension enhances the ability of fabric to resist shear deformation before the shear angle approaches to  $40^\circ$ . While, the increase of shear force is not pronounced when shear angle is larger than  $40^\circ$ , indicating that the pre-tension hardly affect the shear force when the studied woven fabric is sheared to densification. This phenomenon is important to analyze the shear pre-tension coupling behavior of woven fabric in the forming process of large shear deformation.

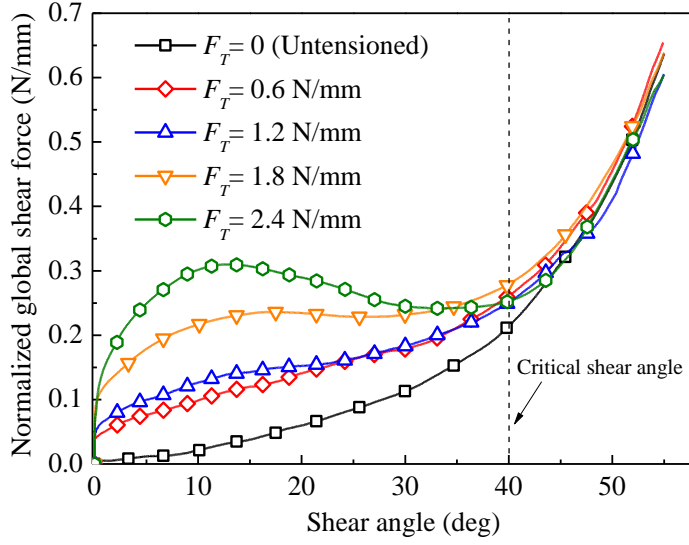


**Fig. 8** Normalized shear force versus shear angle curves under different pre-tensions.

Here, it is important to compare the shear forces which are affected by different pre-tension levels. According to the literature [26], a coupling factor  $CF$  is defined as:

$$CF(\lambda) = \frac{F_{NS,P}(\lambda)}{F_{NS,0}(\lambda)}, \quad (3)$$

where  $F_{NS,P}$  is the normalized shear force with pre-tension, and  $F_{NS,0}$  is the normalized shear force without pre-tension. The coupling factor  $CF$  under different pre-tension levels is characterized in Fig. 9. Before  $40^\circ$  shear angle, as increase the pre-tension levels, the amplitude and slope of the  $CF$  curves rise, indicating the enhancement of pre-tension can improve the ability of the fabric to resist shear deformation. On the other hand, with the evolution of the shear angle, the  $CF$  curves under different pre-tension levels gradually become consistent, and approach to 1. That is the pre-tension cannot affect the shear force when shear angle is larger than  $40^\circ$ .

Besides, as shown in Fig. 9, at the beginning of shear deformation, the  $CF$  value is dramatically enhanced due to the increase of static friction among yarns when

applying a pre-tension, which was also reported by Zhu's work [32]. Then, considering the enhancement of interaction force among yarns can reduce the evolution of fabric surface due to the fabric weaving structure. Thus, in order to explore the effect of the pre-tension on the interaction force among yarns, the evolution of un-sheared fabric surface under different pre-tensions was calculated through the software Vic 3D as shown in Fig. 10. The Z-coordinate of the fabric surface decreases with the increasing pre-tension. The maximum amplitudes are 1.14 mm, 0.73 mm, 0.69 mm, 0.65 mm for pre-tension level of 0.6 N/mm, 1.2 N/mm, 1.8 N/mm, 2.4 N/mm, respectively, indicating the interaction force is enhanced. Obviously, the variation of surface is not significant when pre-tension is higher than 1.2 N/mm. While, the interaction force should be still increased remarkably as described of the static friction enhancement among yarns in Fig. 9, suggesting the deformation of yarn becomes difficult.

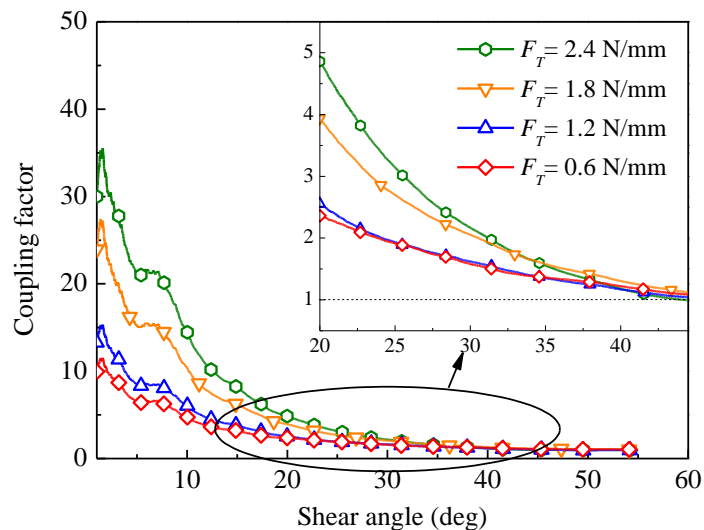


**Fig. 9** The coupling factors with the evolution of shear angle under different levels of pre-tension.

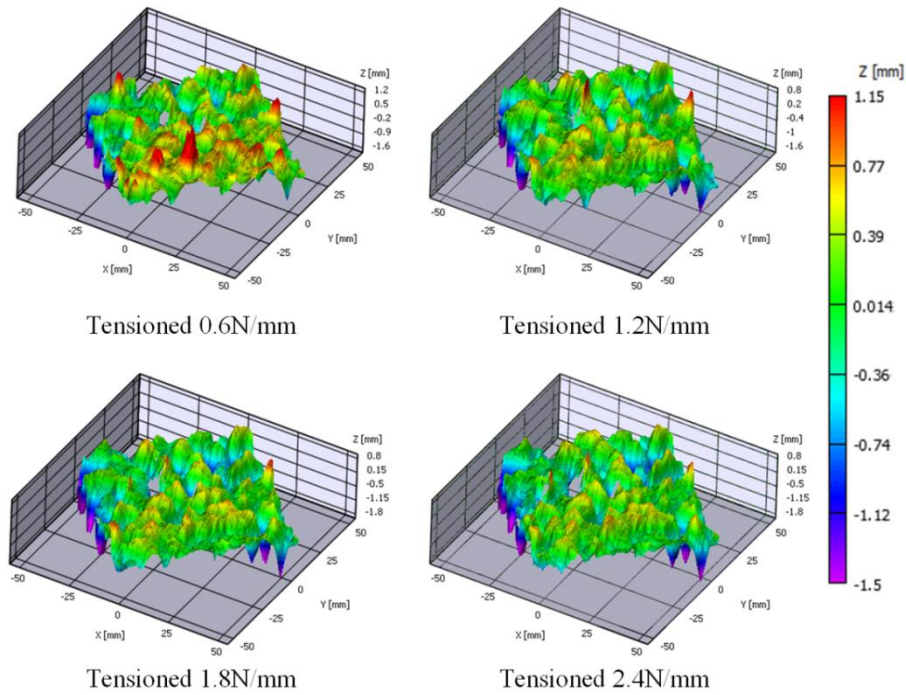


**Fig. 10** Contours plots of the measured distribution of the deformation of the fabric surface along the normal direction to the fabric surface under different pre-tension levels.

### 3.3 Variation of yarn width

As shown in Fig.11, generally, in the view of mesoscopic scale, there are three typical deformation stages in shear deformation of woven fabrics [11]. The yarns firstly rotate with each other until the yarn gaps disappear. Then, the yarns rotate without the gaps and suffer both lateral and longitudinal compression. Local buckling of the yarns will also arise. Finally, the yarns reach a compression limit (shear locking). Beyond the shear locking angle, the yarns primarily experience lateral compression, and the in-plane shear deformation is not pure. The yarn width continues to decrease, leading to the out of plane waviness of fibers, namely, the appearance of wrinkle defect. Thus, obviously, the variation of the yarn width in the

shear process, as a most important mesoscopic feature, is a significant index to reflect the different stages of shear deformation. Most importantly, the variation of the yarn with under different levels of pre-tension can clearly index the effect of shear pre-tension coupling effect.

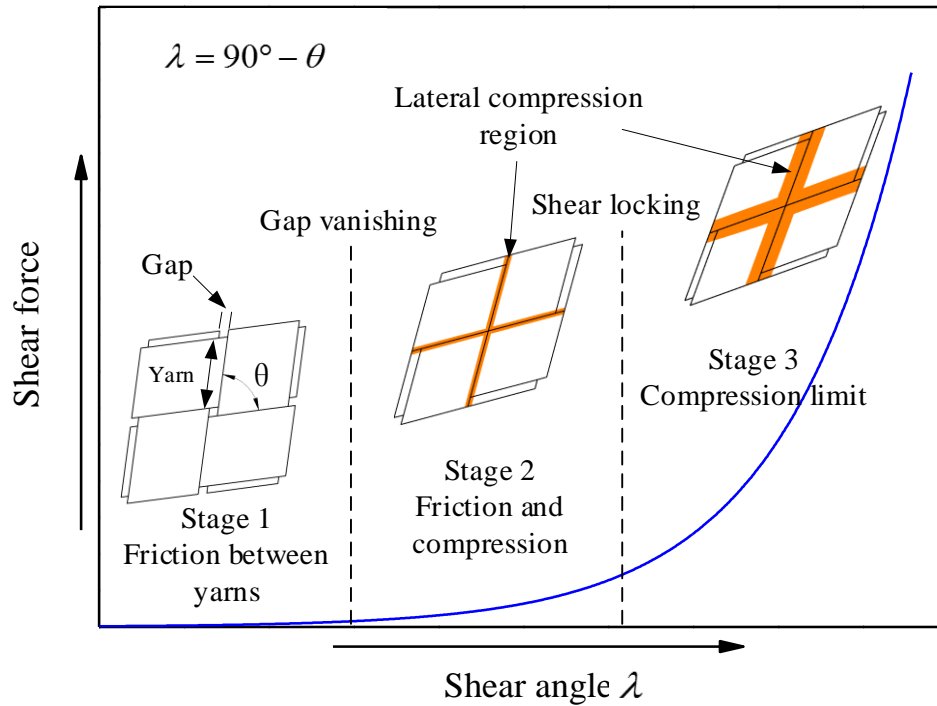


**Fig. 11** Three stages of shear deformation for woven fabric. Stage1: yarns rotation. Stage 2: rotation and lateral and longitudinal compression of yarns. Local buckling of the yarns will also arise. Stage3: reaching compression limit and wrinkle defect arise.

The yarn widths  $w(\lambda)$  under different pre-tension levels are given in Fig. 12a. As the arrangement of this woven fabric yarns is tight, the variation of yarn width in the first stage of shear deformation, namely, small value of shear angle, is not pronounced. Consistent with the yarn width variation under condition of no pre-tension in the literature [11], with or without pre-tension, the yarn width shows a decreasing trend when the shear angle increases. While, the  $w(\lambda)$  under different

pre-tension levels shows clear enhancements at the same shear angle compared with that with no pre-tension. For instance, the  $w(\lambda)$  is increased by 0.07 at the shear angle of  $42^\circ$  for 0.6 N/mm pre-tension, indicating the previous conclusions with regard to the yarn evolution under no pre-tension are not appropriate for that of under specific pre-tension. Then, in order to explore the effect of pre-tension on the yarn width variation, the variation of yarn width  $\Delta w(\lambda)$  is presented in Fig. 12b, and the value is calculated by:

$$\Delta w(\lambda) = w(0^\circ) - w(\lambda), \quad (4)$$

where the  $w(0^\circ)$  is the yarn width of un-sheared fabric. It is remarkable that  $\Delta w(\lambda)$  decreases with the increasing pre-tension, suggesting that the pre-tension suppresses the lateral compression deformation of yarn. Especially, the suppression effect becomes remarkable with the enlarged shear angle. Actually, the reduction of  $\Delta w(\lambda)$  with the enlarged pre-tensions will decrease the deformation in thickness direction of yarn. Therefore, this result confirms that the pre-tension can suppress the wrinkle defect which is always induced by large deformation in thickness direction of yarn. It can be seen that the  $\Delta w(\lambda)$  is hard to be distinguished when pre-tension is higher than 1.2N/mm, indicating that the effect of pre-tension to suppress wrinkle defect cannot be unlimitedly improved. These results also reflect that the serious wrinkle defects induced by excessive shear deformation can be controlled by applying pre-tension, but cannot be unlimitedly suppressed by solely improving the level of pre-tension in the practical forming process.

In order to predict the yarn width evolution of the comingled

glass-polypropylene 2-2 twill woven fabric under different pre-tension level, a model  $w(\lambda, F_T)$  considering pre-tension effect is proposed based on the reported work [11], and it is given as:

$$w(\lambda, F_T) = w(0^\circ) \cdot \cos(A \cdot \lambda), \quad (5)$$

where the parameter  $A$  is the effect factor of the pre-tension. To simplify the equation, the concept of width variation ratio  $r = w(\lambda, F_T)/w(0^\circ)$ , which is the transformation of Eq. (5), is used here. As shown in Fig. 13a, the measured data of  $r$  versus shear angle is fitted by the model. The effect factor of parameters  $A$  under different pre-tension levels can be also obtained, and is listed in Table 2. The high value of correlation factor Adj (R2) demonstrates the fitting effectiveness of the model. That is the model can effectively capture the yarn width evolution.

**Table 2** The values of correlation factor Adj (R2) and parameter  $A$ .

$F_T(\text{N/mm})$	0	0.6	1.2	1.8	2.4
Adj (R2)	0.958	0.968	0.937	0.981	0.975
$A$	0.828	0.782	0.703	0.694	0.696

In order to explore the effects of pre-tension on the  $w(\lambda, F_T)$ , the values of parameter  $A$  obtained in this work versus pre-tension level are plotted as scatters in the Fig. 13b, and the values are fitted by exponential function by using the least square method:  $A = 0.670e^{(-0.102F_T)} + 0.163e^{(-0.957F_T)}$  in data analysis software Origin. The correlation factor Adj (R2) is 0.88, suggesting the exponential function can effectively predict the variation of parameters  $A$  under the pre-tension range of 0.0-2.4N/mm. It can be seen that the parameter  $A$  is reduced with the increasing of pre-tension level.

While, the slope of parameter  $A$  curve decreases, indicating the effects of pre-tension on the yarn width variation gradually weaken. Then, substitute the exponential function into Eq. (5), the yarn width  $w(\lambda, F_T)$  when the fabric suffer shear deformation under pre-tension can be expressed as:

$$w(\lambda, F_T) = w(0^\circ) \cdot \cos\left(\left(0.670e^{(-0.102F_T)} + 0.163e^{(-0.957F_T)}\right) \cdot \lambda\right), 0 \leq F_T \leq 2.4N / \text{mm}. (6)$$

Thus, in view of mesoscopic scale, Eq. (6) can capture the evolution of yarn width under different shear angle and especially under pre-tensions. That is the yarn width under shear pre-tension coupling can be predicted for the comingled glass-polypropylene 2-2 twill woven fabric. In addition, according to the Eq. (5), the parameter  $A$  has a non-linear dependence with the shear behavior when the shear angle is kept constant as shown in Fig 14a. While, as the effective interval of parameter  $A$  is limited by the applied pre-tension as shown in the Fig. 13b, the non-linear relationship is not significant in the effective interval of this work (Fig. 14b). With the decreasing of parameter  $A$ , the yarns width is enlarged, indicating the yarn width variation  $\Delta w(\lambda) = w(0^\circ) - w(\lambda)$  is suppressed. While, the increase trend of  $w(\lambda)$  is gradually reduced as the decreasing of parameter  $A$ . Moreover, with the increasing of shear angle, the effect of parameter  $A$  on the yarn width  $w(\lambda)$  is remarkably improved. For instance, the variations of  $w(\lambda)$  in the range of parameter  $A$  from 0.696 to 0.826 are 0.013, 0.050, 0.110, 0.192 and 0.292 for the shear angle of  $10^\circ$ ,  $20^\circ$ ,  $30^\circ$ ,  $40^\circ$  and  $50^\circ$ , respectively.

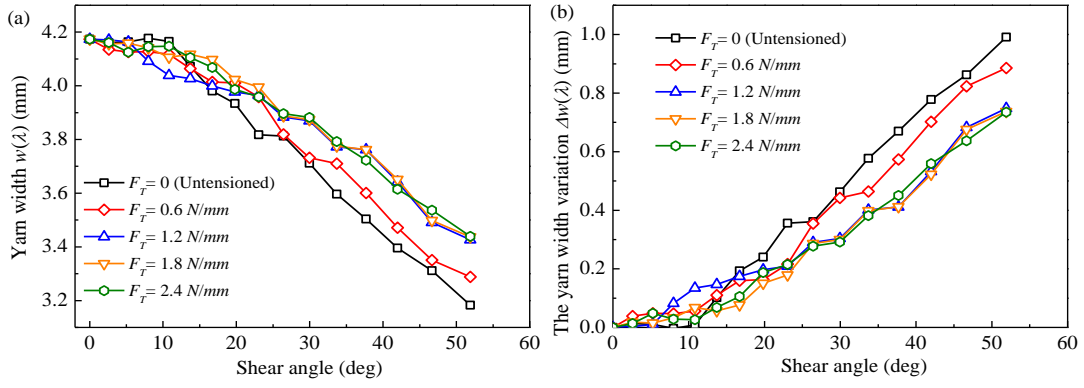


**Fig. 12** (a) Yarn width  $w(\lambda)$  versus shear angle and (b) the variation of yarn width  $\Delta w(\lambda)$  versus shear angle under different pre-tension levels.

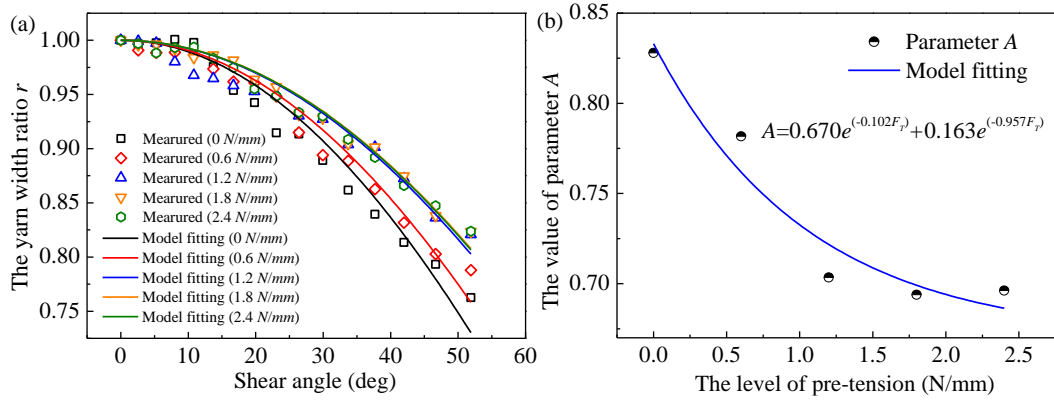


**Fig. 13** (a) The measured yarn width ratio  $r$  and modeling fitting under different pre-tension levels. (b) The effect factor  $A$  and fitting model versus the different level of pre-tension.

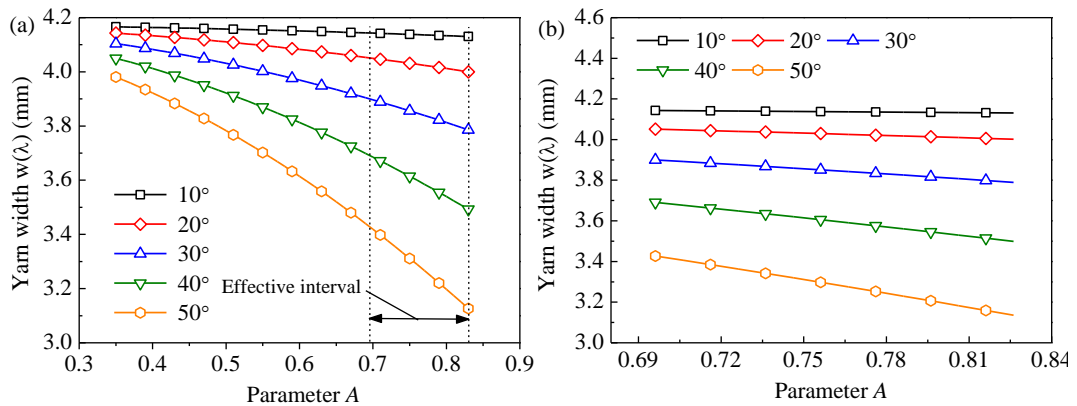


**Fig. 14** (a) The non-linear relationship between yarn width and the parameter  $A$ ; (b) the yarn width versus the parameter  $A$  curves in the effective interval.

## **4 Discussion**

### **4.1 Macroscopic shear performance**

In this work, the shear force of the comingled glass-polypropylene 2-2 twill woven fabric shows an evident increase when subjected to pre-tension, as pre-tension enhances the friction between yarns. However, the improvement of shear force is not obvious when the shear angle is larger than  $40^\circ$ . This convergence phenomenon of curves in Fig. 8 is also reported in studies [23, 27], and up to now, these works believe that this result is owing to the inherent design limitation of the test device, which causes a relaxation of the pre-tension force applied to the fabric force when the shear deformation is enlarged to specific degree. However, for the devised picture frame fixture in current work, the pre-tension provided by springs will not be relaxed in experiment. Actually, when the fabric reached a specific shear angle (about  $40^\circ$  in this work, i.e. stage 3), the gaps among yarns and the gaps among fibers disappeared, and the deformation approached to be no-pure in-plane shear as described in the Fig. 6 and 7. Besides, when the shear angle is larger than critical value, such as  $40^\circ$  in this work, the yarns rotation was largely limited, and the lateral compression was primary deformation mode of the fabrics. Thus, the shear deformation of the densified fabrics can be regarded as the deformation of an entity without gaps, making the shear force almost unaffected by pre-tension.

### **4.2 Mesoscopic deformation**

As shown in Fig. 10 and 12, the pre-tension has significant effect on the mesoscopic geometric features of the fabric. However, when the pre-tension is above

1.2 N/mm, this effect is not remarkable. As shown in Fig. 15, the normal pressure between the surfaces of two yarns is enhanced when yarns are subjected to pre-tension, and will also result in a reduction in the cross-sectional height of the yarns. Thus, the undulation of the fabric surface will decrease. However, with the increasing of deformation degree of the yarn cross section, the degree of deformation difficulty is enlarged exponentially [33]. Thus, the effect of pre-tension on reduction of the undulation of fabric surface is not significant when the value of pre-tension is higher than 1.2N/mm (Fig. 10).As shown in Fig. 15, the fibers in the yarns will be arranged more closely as cross-sectional height of the yarn decreases, indicating that the ability of yarn to resist lateral compression is enhanced. Thus, the variation of the yarn width  $\Delta w(\lambda)$  is reduced when subjected to pre-tension. While, the  $\Delta w(\lambda)$  approaches to be constant when the pre-tension is larger than 1.2N/mm, since the cross-sectional height of yarn can be hardly changed more.

It is well know that the  $\Delta w(\lambda)$  is a significant cause of wrinkle appearance, since the yarn width reduction will lead to the increase of the yarn thickness, and the nature of the wrinkle defect is the over increase of the yarn thickness [11]. That is the relative large  $\Delta w(\lambda)$  will lead to the significant increase of the yarn thickness, and the wrinkle defect will arise more easily. In this work, when the pre-tension is applied on the yarns, we experimentally identify that at the same shear angle, the yarn width reduction  $\Delta w(\lambda)$  is much lower compared with that of without pre-tension as shown in Fig. 12. For instance, the  $\Delta w(\lambda)$  is lowered by 0.07 at the shear angle of  $42^\circ$  for 0.6 N/mm pre-tension compared with that without pre-tension. Thus, this indicates

that the pre-tension effectively suppresses the yarn width reduction, namely, suppresses the fiber movement in the thickness direction. Consider the relationship between the arise of the wrinkle defect and the yarn width reduction, it can be concluded that the pre-tension can suppress wrinkle defects.

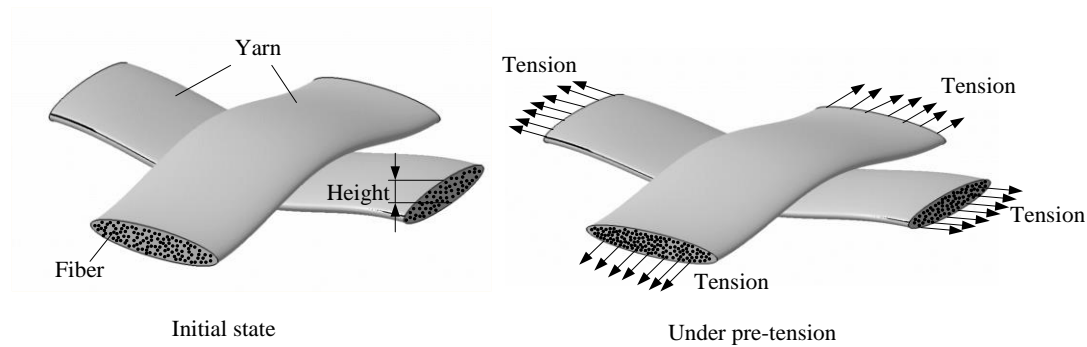


**Fig. 15** Diagram of the yarn deformation under pre-tension.

## 5 Conclusions

This work focuses on the shear pre-tension coupling behavior of comingled glass-polypropylene 2-2 twill woven fabric in macro and mesoscopic scale. A self-developed picture frame fixture was designed to implement shear experiments. The effects of pre-tension on macro shear force and mesoscopic features, including undulation of fabric surface and variation of yarn width, were obtained and discussed. Main conclusions are summarized as follows:

- (1) A picture frame fixture was originally designed with a concise approach to apply pre-tension for testing shear pre-tension coupling behavior. The experimentally obtained shear deformation under applied pre-tension is uniform, demonstrating the effectiveness and reliability of the self-developed picture frame fixture.
- (2) The critical shear angle of the comingled glass-polypropylene 2-2 twill woven fabric is experimentally confirmed to be  $40^\circ$ , and the in-plane shear deformation is

not pure when shear angle is higher than  $40^\circ$ . The shear force is enhanced significantly by increasing pre-tension when the shear angle is lower than  $40^\circ$ . While, the shear force can not be enhanced when shear angle is beyond  $40^\circ$ .

- (3) The pre-tension suppresses the mesoscopic undulation of un-sheared fabric surface, suggesting the enhancement of coupling effect at the initiation of shear deformation due to the static friction. However, the suppression effect on the undulation is not obvious when the pre-tension is higher than 1.2N/mm.
- (4) The enlarged shear angle leads to the reduction of Yarn width. With the increasing pre-tension, the variation of yarn width  $\Delta w(\lambda)$  is reduced, since the pre-tension enhances the ability to resist lateral deformation. While, the  $\Delta w(\lambda)$  approaches to be constant when pre-tension is higher than 1.2N/mm.

In the future work, relative large shear angle of the picture frame fixture should be designed to induce obvious wrinkle defects, so that the correlations among the pre-tensions, yarn width evolution and wrinkle defects can be further revealed.

### **Acknowledgements**

This work is supported by National Natural Science Foundation of China (Grant No. 51621004, 51875187 and 11972154), Hunan Province Science and Technology Plan (Grant No. 2019JJ40021), and Shenzhen Science Innovation Committee Foundation (Grant No. JCYJ20160530193728307). This work is also supported by the Fund of State Key Laboratory of Structural Analysis for Industrial Equipment under grant #GZ18106.

## Data Availability Statement

All data obtained or analyzed in this work are included in this manuscript.

## References

- [1] Liu Q, Lin Y, Zong Z, Sun G, Li Q. Lightweight design of carbon twill weave fabric composite body structure for electric vehicle. *Compos Struct* 2013;97:231-238.
- [2] Mo F, Zhang H, Yang X, Duan S, Xiao Z. Coupling investigation on tensile and acoustic absorption properties of lightweight porous LGF/PP composite. *Polym Compos* 2018;40(4):1315-1321.
- [3] Wei K, Liang D, Mei M, Yang X, Chen L. A viscoelastic model of compression and relaxation behaviors in preforming process for carbon fiber fabrics with binder. *Compos B Eng* 2019;158:1-9.
- [4] Wei K, Yang QD, Yang XJ, Tao Y, Xie HQ, Qu ZL, Fang DN. Mechanical analysis and modeling of metallic lattice sandwich additively fabricated by selective laser melting. *Thin Walled Struct.* 2020; 146: 106189.
- [5] Do TT, Lee D-J. Effects of the wrinkled fabric preform on the bending properties of resin transfer molded composites. *J Mater Sci* 2009;44(16):4219-4227.
- [6] Wei K, Yang QD, Yang XJ, Xie HQ, Qu ZL, Fang DN. Mechanical properties of Invar 36 alloy additively manufactured by selective laser melting. *Mater. Sci. Eng.* 2020; 772: 138799.
- [7] Boisse P, Hamila N, Vidal-Sallé E, Dumont F. Simulation of wrinkling during textile composite reinforcement forming. Influence of tensile, in-plane shear and

- bending stiffnesses. *Compos Sci Technol* 2011;71(5):683-692.
- [8] Tephany C, Gillibert J, Ouagne P, Hivet G, Allaoui S, Soulat D. Development of an experimental bench to reproduce the tow buckling defect appearing during the complex shape forming of structural flax based woven composite reinforcements. *Compos A Appl Sci Manuf* 2016;81:22-33.
- [9] Wang P, Legrand X, Boisse P, Hamila N, Soulat D. Experimental and numerical analyses of manufacturing process of a composite square box part: Comparison between textile reinforcement forming and surface 3D weaving. *Compos B Eng* 2015;78:26-34.
- [10] Boisse P, Hamila N, Guzman-Maldonado E, Madeo A, Hivet G, dell'Isola F. The bias-extension test for the analysis of in-plane shear properties of textile composite reinforcements and prepregs: a review. *Int J Mater Form* 2016;10(4):473-492.
- [11] Zhu B, Yu T, Tao X. An experimental study of in-plane large shear deformation of woven fabric composite. *Compos Sci Technol* 2007;67(2):252-261.
- [12] Hosseini A, Kashani MH, Sassani F, Milani AS, Ko FK. Identifying the distinct shear wrinkling behavior of woven composite preforms under bias extension and picture frame tests. *Compos Struct* 2018;185:764-773.
- [13] Guzman-Maldonado E, Wang P, Hamila N, Boisse P. Experimental and numerical analysis of wrinkling during forming of multi-layered textile composites. *Compos Struct* 2019;208:213-223.
- [14] Kim J-I, Hwang Y-T, Choi K-H, Kim H-J, Kim H-S. Prediction of the vacuum

- assisted resin transfer molding (VARTM) process considering the directional permeability of sheared woven fabric. *Compos Struct* 2019;211:236-43.
- [15] Pierce RS, Falzon BG, Thompson MC. Permeability characterization of sheared carbon fiber textile preform. *Polym Compos* 2016;39(7):2287-2298.
- [16] Gereke T, Döbrich O, Hübner M, Cherif C. Experimental and computational composite textile reinforcement forming: A review. *Compos A Appl Sci Manuf* 2013;46:1-10.
- [17] Bussetta P, Correia N. Numerical forming of continuous fibre reinforced composite material: A review. *Compos A Appl Sci Manuf* 2018;113:12-31.
- [18] Krogh C, White KD, Sabato A, Sherwood JA. Picture-frame testing of woven prepreg fabric: An investigation of sample geometry and shear angle acquisition. *Int J Mater Form* 2019;1-13.<https://doi.org/10.1007/s12289-019-01499-y>
- [19] Cao J, Akkerman R, Boisse P, Chen J, Cheng HS, de Graaf EF, et al. Characterization of mechanical behavior of woven fabrics: Experimental methods and benchmark results. *Compos A Appl Sci Manuf* 2008;39(6):1037-1053.
- [20] Haghi Kashani M, Hosseini A, Sassani F, Ko FK, Milani AS. The Role of Intra-Yarn Shear in Integrated Multi-Scale Deformation Analyses of Woven Fabrics: A Critical Review. *Crit Rev Solid State Mater Sci* 2017;43(3):213-232.
- [21] Montazerian H, Rashidi A, Hoorfar M, Milani AS. A frameless picture frame test with embedded sensor: Mitigation of imperfections in shear characterization of woven fabrics. *Compos Struct* 2019;211:112-124.

- [22] Rashidi A, Milani AS. Passive control of wrinkles in woven fabric preforms using a geometrical modification of blank holders. *Compos A Appl Sci Manuf* 2018;105:300-309.
- [23] Matveev MY, Endruweit A, De Focatiis DSA, Long AC, Warrior NA. A novel criterion for the prediction of meso-scale defects in textile preforming. *Compos Struct* 2019;226:111263.
- [24] Tavana R, Najar SS, Abadi MT, Sedighi M. Meso/macro-scale finite element model for forming process of woven fabric reinforcements. *J Compos Mater* 2012;47(17):2075-2085.
- [25] Nosrat Nezami F, Gereke T, Cherif C. Analyses of interaction mechanisms during forming of multilayer carbon woven fabrics for composite applications. *Compos A Appl Sci Manuf* 2016;84:406-416.
- [26] Chen S, Harper LT, Endruweit A, Warrior NA. Formability optimisation of fabric preforms by controlling material draw-in through in-plane constraints. *Compos A Appl Sci Manuf* 2015;76:10-19.
- [27] Harrison P, Gomes R, Curado-Correia N. Press forming a 0/90 cross-ply advanced thermoplastic composite using the double-dome benchmark geometry. *Compos A Appl Sci Manuf* 2013;54:56-69.
- [28] Willems A, Lomov SV, Verpoest I, Vandepitte D. Picture frame shear tests on woven textile composite reinforcements with controlled pretension. In: *Proceedings of 10th ESAFORM conference on material forming*. Zaragoza; May, 2007. p. 999–1004.

- [29] Launay J, Hivet G, Duong AV, Boisse P. Experimental analysis of the influence of tensions on in plane shear behaviour of woven composite reinforcements. *Compos Sci Technol* 2008;68(2):506-515.
- [30] Nosrat-Nezami F, Gereke T, Eberdt C, Cherif C. Characterisation of the shear-tension coupling of carbon-fibre fabric under controlled membrane tensions for precise simulative predictions of industrial preforming processes. *Compos A Appl Sci Manuf* 2014;67:131-139.
- [31] Kashani MH, Rashidi A, Crawford BJ, Milani AS. Analysis of a two-way tension-shear coupling in woven fabrics under combined loading tests: Global to local transformation of non-orthogonal normalized forces and displacements. *Compos A Appl Sci Manuf* 2016;88:272-285.
- [32] Zhu D, Mobasher B, Vaidya A, Rajan SD. Mechanical behaviors of Kevlar 49 fabric subjected to uniaxial, biaxial tension and in-plane large shear deformation. *Compos Sci Technol* 2013;74:121-30.
- [33] Wei K, Liang D, Mei M, Wang D, Yang X, Qu Z. Preforming behaviors of carbon fiber fabrics with different contents of binder and under various process parameters. *Compos B Eng* 2019;166:221-232.